

Silent white light: Reduction of the second-order intensity correlation coefficient

Kai Niklas Hansmann ^{1,*}, Franziska Dommermuth,¹ Wolfgang Elsässer ^{1,2,3} and Reinhold Walser ¹

¹*Technical University of Darmstadt, Institute of Applied Physics, Hochschulstrasse 4a, D-64289 Darmstadt, Germany*

²*School of Physics, Trinity College Dublin, Dublin 2 D02PN40, Ireland*

³*Istituto di Elettronica e di Ingegneria dell'Informazione e delle Telecomunicazioni (IEIT) del Consiglio Nazionale delle Ricerche (CNR), Politecnico di Torino, 10129 Torino, Italy*



(Received 13 October 2023; accepted 24 June 2024; published 31 July 2024)

We investigate the intrawaveguide statistics manipulation of broadband light by combining semiconductor quantum dot physics with quantum optics. By cooling a quantum dot superluminescent diode to the liquid nitrogen temperature of 77 K, Blazek *et al.* [*Phys. Rev. A* **84**, 063840 (2011)] have demonstrated a temperature-dependent reduction of the second-order intensity correlation coefficient from 2 for thermal amplified spontaneous emission light to $g^{(2)}(0, T = 190 \text{ K}) \approx 1.33$. Here, we model the broadband photon statistics assuming amplified spontaneous emission radiation in a pumped, saturable quantum dot gain medium. We demonstrate that, by an intensity increase due to the quantum dot occupation dynamics via the temperature-tuned quasi-Fermi levels, together with the saturation nonlinearity, a statistics manipulation from thermal Bose-Einstein statistics towards Poissonian statistics can be realized, thus producing “silent white light” with a reduced second-order correlation coefficient. Such intensity-noise-reduced broadband radiation is relevant for many applications such as optical coherence tomography, optical communication, or optical tweezers.

DOI: [10.1103/PhysRevResearch.6.L032025](https://doi.org/10.1103/PhysRevResearch.6.L032025)

The quantum fluctuations of light have been in the center of research interests since the first realization of the laser, driven by both fundamental and practical interests [1]. This can be best summarized by the famous saying of Landauer: “The noise is the signal” [2]. In this spirit, lasers and thermal light sources as “original light sources” have been considered as benchmarks due to their second-order correlation coefficient $g^{(2)}(0) = \langle I^2 \rangle / \langle I \rangle^2$ of unity and 2, respectively [3], determined within a Hanbury Brown and Twiss (HBT) experiment [4,5]. Nowadays, a HBT classification in the $g^{(2)}(0)$ scheme is the characteristics for each new light source and has become central to quantum optical measurements.

Immediately after the advent of the laser, Martienssen and Spiller and Arecchi [6,7] realized the so-called pseudo-thermal light source in 1966. There, the scattering of laser light at a rotating diffuser transformed the Poissonian laser photon statistics into that of thermal light [8,9] exhibiting Bose-Einstein statistics with $g^{(2)}(0)$ of 2. This concept of generating light with super-Poissonian statistics, i. e., bunched or even superbunched photon counting statistics, by exploiting Gaussian and non-Gaussian random walk scattering processes in media led to the achievement of well-controlled states of light [10–15]. Later on, further microscopic and mesoscopic scattering concepts for the manipulation of light statistics have

been comprehensively investigated and extended to waveguides [16–19].

Very recently, it has been shown that disordered systems permit manipulation and tuning of the statistics via deterministic and coherent control. Monochromatic coherent light traversing a disordered photonic medium evolved into a random field whose statistics has been dictated by the disorder level [18,20]. Deterministic control over the photon-number distribution was demonstrated by interfering two coherent beams within a disordered photonic lattice, thus enabling the generation of superthermal and subthermal light [21].

The generation of sub-Poissonian statistics of light states [22] with $g^{(2)}(0)$ below 1 and even single photon states by means of nonlinear optics have been the next revolutionary steps and opened a huge field of applications in sensing [23–28]. A particularly interesting emission statistics of optoelectronic semiconductor-based emitters can be created by the method of “quiet pumping” pioneered by Yamamoto. By transferring the, by Coulomb repulsion regulated, sub-Poissonian statistics of the quiet injection current onto the statistics of the emitted photons, sub-Poissonian states of light emerge [29–31]. The concept of manipulating light states and exploiting their novel statistical properties beneficially via tailoring $g^{(2)}(0)$ on demand in quantum metrology applications has also been investigated by applying nonlinear optical processes onto light [32,33].

More recently, even so-called hybrid light has been discovered by Blazek *et al.* [34] by investigating the emission properties of quantum dot superluminescent diodes (QDSLs). At room temperature, those are light sources with an ultrabroadband emission spectrum (first-order coherence) and a second-order correlation coefficient $g^{(2)}(0) = 2.0$

*Contact author: kai.hansmann@physik.tu-darmstadt.de

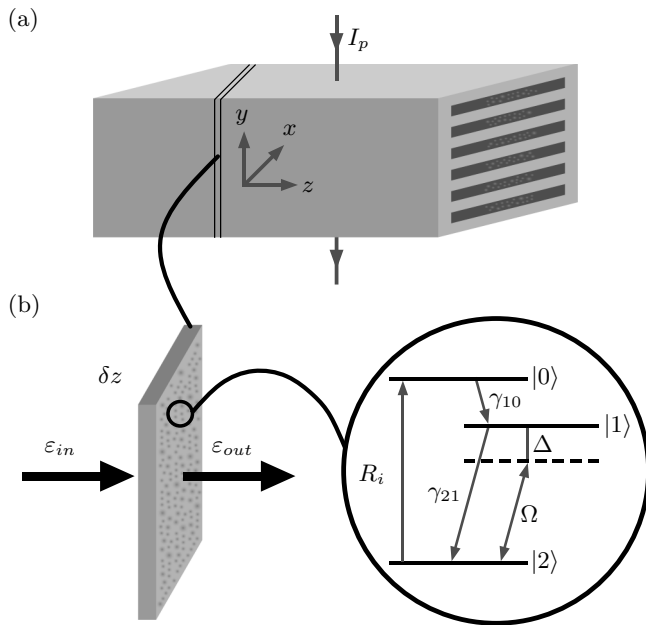


FIG. 1. (a) QDSL pumped by an electric injection current I_p . Layers of waveguides with nonreflecting tilted end facets and embedded QDs serve as a lossy, nonlinear gain material. (b) Stochastic electric field $\varepsilon(t)$ propagating for a length δz through a transversal sheet of inverted three-level QDs with decay rates γ_{10} , γ_{21} , an internal pumping rate R_i , a Rabi frequency Ω , and a detuning Δ .

[35–37]. However, Blazek *et al.* [34] demonstrated experimentally, that the intensity fluctuations can be suppressed down to $g^{(2)}(0) = 1.33$ while tuning the temperature to 190 K. Such emission, being first-order incoherent (spectrally broadband) and second-order coherent (towards that of a laser), might be called “silent white light” and is of particular interest for applications such as optical coherence tomography [38], fiber optic gyroscope [39], and ghost imaging [40,41].

Our approach here is not by reconstructing the quantum optical state of silent white light as has been performed in Refs. [42–44], but rather more by deriving an expression for $g^{(2)}(0)$ based solely on the practical aspects for quantum metrology. In this spirit, we present a quantitative model for explaining this tailoring of $g^{(2)}(0)$ [34] from the “standard $g^{(2)}(0) = 2.0$ ” value for thermal amplified spontaneous emission (ASE) sources [45] towards a value of 1.33. Our model accounts for the self-consistent modification of the photon statistics caused by the nonlinear response of the QD gain medium [46], as well as thermally induced occupation of its energy levels [47,48]. This insight will promote further developments of compact and fully integrated light sources. For example, state-of-the art applications range from optical coherence tomography [37,38,49], white light interferometry [50–52], control of chemical kinetics with tailored incoherent light [53], to sensing with fiber optic gyroscopes [54,55].

Radiation is generated in an active QD gain medium by ASE. In contrast to a laser, the waveguide medium is terminated with nonreflecting tilted end facets, shown in Fig. 1(a). The equilibrium state of the radiation inside the diode is a balance between the nonlinear gain from the QD ensemble, its saturation behavior, the absorption from the passive medium, and the emission output coupling of the diode. In the

following, these processes are considered in detail for a thin transversal layer of QDs interacting with the radiation field.

According to the Maxwell-Bloch equations [56,57], the slowly varying electric field amplitude $\varepsilon(t)$ passing through a thin sheet δz of polarizable matter [see Fig. 1(b)] reads

$$\varepsilon_{\text{out}}(t) = \eta \varepsilon_{\text{in}}(t) + \frac{ik\delta z}{2\varepsilon_0} \mathcal{P}^{(+)}(t). \quad (1)$$

Here, $0 < \eta < 1$ accounts for scattering losses, k is the carrier wave number of the electric field, and $\mathcal{P}^{(+)}$ is the positive frequency part of the polarization. QDs are the active agents embedded in the passive waveguide layers inside the diode. They are modeled as pumped three-level systems [see the inset in Fig. 1(b)].

The electric field drives the transition between levels $|1\rangle$ and $|2\rangle$ with Rabi frequency $\Omega(t) = d_{21}\varepsilon(t)/\hbar$, where d_{21} is the dipole matrix element. The positive frequency part of the polarization $\mathcal{P}^{(+)} = nd_{12}\rho_{21}$ scales with the density of QDs n . In the rate equation limit [56], coherences ρ_{ij} decay much faster than populations ρ_{ii} , which evolve as

$$\begin{aligned} \dot{\rho}_{00} &= -(R_i + \gamma_{10})\rho_{00} + R_i\rho_{22}, \\ \dot{\rho}_{11} &= \gamma_{10}\rho_{00} - (\gamma_{21} + \zeta)\rho_{11} + \zeta\rho_{22}, \\ \dot{\rho}_{22} &= R_i\rho_{00} + (\gamma_{21} + \zeta)\rho_{11} - (R_i + \zeta)\rho_{22}, \end{aligned} \quad (2)$$

where $\zeta = |\Omega|^2 \mathcal{L}/\gamma$, $\gamma = \gamma_{21} + R_i$, and $\mathcal{L} = (\gamma/2)^2/[\Delta^2 + (\gamma/2)^2]$. In this limit, the coherence $\rho_{21} = -(i/2)\Omega \mathcal{D} w$ is related to the inversion $w = \rho_{11} - \rho_{22}$ and the stochastic field amplitude $\varepsilon(t)$, which is modulated by the line shape $\mathcal{D} = 1/(i\Delta + \gamma/2)$.

The relaxation times of the atomic populations are assumed to be much shorter than the correlation time of the fluctuations of $\varepsilon(t)$. Therefore, the populations of the QD levels are in instantaneous equilibrium. Hence, the stationary solution of Eq. (2) can be used to determine the instantaneous atomic coherence as

$$\rho_{21} = -\frac{i}{2} \Omega \frac{w_0 \mathcal{D}}{1 + s}, \quad (3)$$

with the unsaturated inversion $w_0 = [R_i(\gamma_{10} - \gamma_{21}) - \gamma_{10}\gamma_{21}]/(\gamma\gamma_{10} + 2R_i\gamma_{21})$. We denote the saturation parameter $s = \mathcal{L}I/I_s$ as the ratio of intensity $I = |\varepsilon|^2$ and the saturation intensity $I_s = \hbar^2\gamma(\gamma\gamma_{10} + 2R_i\gamma_{21})/|d_{21}|^2(3R_i + 2\gamma_{10})$.

Now, the input-output relation from Eq. (1) reads $\varepsilon_{\text{out}} = (\eta + \alpha)\varepsilon_{\text{in}}$ and depends on a nonlinear absorption coefficient $\alpha = \kappa\gamma\mathcal{D}/(1 + s)$, the nonlinear saturation parameter $\kappa = \alpha_0 k\delta z$, and the linear, resonant absorption coefficient $\alpha_0 = n|d_{21}|^2 w_0/4\hbar\varepsilon_0\gamma$ [57]. In the limit of a thin sheet of length δz , all terms exceeding linear order in κ can be neglected and the input-output relation for the intensities is obtained,

$$I_{\text{out}}(I_{\text{in}}) = \left(\eta^2 + \frac{4\eta\kappa}{1 + s} \right) I_{\text{in}} + O[\delta z^2]. \quad (4)$$

As a consequence of the broad THz bandwidth of the first-order incoherent light, we can choose the detuning $\Delta = 0$. Thus, only three parameters η , κ , and I_s remain unspecified in Eq. (4).

Here, we start with an incoherent Gaussian photon statistics as the starting point for the statistics manipulation by the

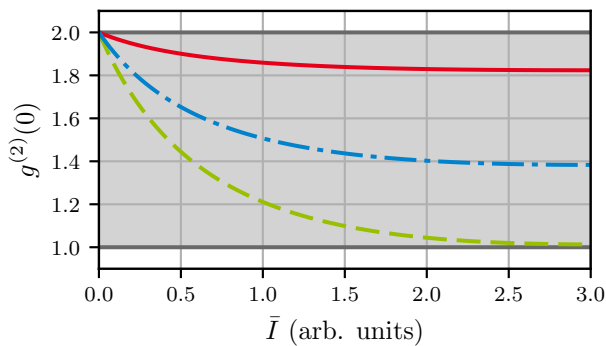


FIG. 2. Second-order correlation coefficient $g^{(2)}(0)$ vs mean intensity \bar{I} , for saturation intensity $I_s = 5$ and three nonlinear saturation parameters $\kappa = 0.1$ (red, solid), 0.35 (blue, dashed-dotted), 0.56 (green, dashed).

QD saturable medium and the QD level scheme. This implies an exponential probability density for the input intensity $p(I_{\text{in}})$ [44],

$$p(I_{\text{in}}) = e^{-I_{\text{in}}/\bar{I}}/\bar{I}, \quad \langle I_{\text{in}} \rangle = \bar{I}, \quad (5)$$

with an average intensity \bar{I} . Thus, the n th-order moments of the output photon intensity are given by

$$\langle I_{\text{out}}^n(I_{\text{in}}) \rangle = \int_0^\infty dI_{\text{in}} I_{\text{out}}^n(I_{\text{in}}) p(I_{\text{in}}). \quad (6)$$

In equilibrium, gain is compensated by loss and defines a self-consistent relation for the intensity (4),

$$\langle I_{\text{out}} \rangle = \langle I_{\text{in}} \rangle = \bar{I}(\eta). \quad (7)$$

From this condition, we can determine the inaccessible loss rate $\eta(\bar{I})$ in favor of the equilibrium intensity \bar{I} .

Now, we are able to evaluate the stationary, zero delay time ($\tau = 0$) relative intensity-noise correlation function

$$g^{(2)}(\tau = 0, \bar{I}) = \lim_{t \rightarrow \infty} \langle I_{\text{out}}(t)^2 \rangle / \langle I_{\text{out}} \rangle^2 \quad (8)$$

as a measure for the intensity fluctuations. Serendipitously, one can evaluate this expression analytically in terms of $u(\mathcal{I}) = e^{\mathcal{I}}\Gamma(0, \mathcal{I})$, the incomplete gamma function $\Gamma(0, \mathcal{I}) = \int_{\mathcal{I}}^\infty dt e^{-t}/t$ [58], and the relative intensity $\mathcal{I} = I_s/\bar{I}$. Within the thin sheet limit $O[\delta z^2]$, one finds in good approximation

$$g^{(2)}(0) = 2 - 8\kappa\mathcal{I}\{1 + \mathcal{I}[1 - 2u(\mathcal{I})] - \mathcal{I}^2u(\mathcal{I})\}. \quad (9)$$

In Fig. 2, we depict this intensity correlation $g^{(2)}(0)$ versus the internal QDSDL intensity \bar{I} for a chosen saturation intensity I_s and various saturation parameters $\kappa = 0.1, 0.35$, and 0.56 , respectively. In general, $g^{(2)}(0)$ shows a strong decrease with increasing \bar{I} , which is stronger for higher κ . However, we note that this is only the case if the medium is inverted, i. e., $\kappa > 0$.

In agreement with previous work on thermal ASE sources [45], we observe $g^{(2)}(0) = 2.0$ for all parameter combinations at low input intensity. Maintaining the balance between gain and loss by implicitly satisfying Eq. (7), increasing saturation in the medium is reached by tuning the internal QDSDL intensity \bar{I} rather than the external pumping rate I_p . Hence, our observation of intensity noise suppression with increasing \bar{I} extends established knowledge on thermal ASE sources [45].

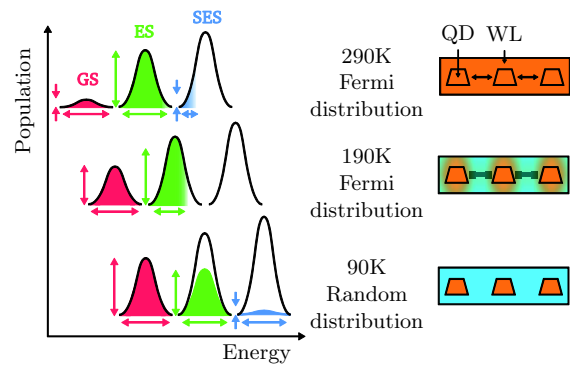


FIG. 3. Schematic depiction of the occupation of the QD levels as a function of temperature T for the explanation of the experimental measurement of peak power emitted by the diode from Ref. [34].

Thermal effects within the QD gain medium influence the carrier population and thus determine the key parameter of $g^{(2)}(0)$ via the generated photon density or the intensity \bar{I} . Its influence on the statistics via the emitted intensity are schematically summarized in Fig. 3. For the description of this temperature-dependent reduced second-order correlation coefficient, we consult a rate equation model that has been developed previously to describe the threshold currents' temperature dependence in strongly inhomogeneously broadened QD lasers, reflecting its radiative recombination processes [47,48]. Thereby, we combine the two worlds of quantum optics and semiconductor quantum dots.

The charge-carrier distribution in semiconductor QD materials depends on temperature, and the mean carrier occupation number for each energy level is obtained by averaging over the whole inhomogeneous dot ensemble. The ingredients of the model are the two confined QD levels, namely the GS (ground state) and the ES (excited state), and the so-called wetting layer, which provides the joint interaction medium for all QDs. Their appropriate interaction is accounted for by relaxation rates, carrier escape processes via thermally activated escape, tunneling, and Auger processes. Finally, all states interact with a bosonic phonon bath. The outcome is the carrier distribution or the population densities entering directly into the radiative photon emission rates.

At room temperature, high-energy phonons induce a global thermal equilibrium of the whole QD ensemble through interaction with the surrounding wetting layer (see Fig. 3). This thermally excites some of the carriers into higher energetic states, leaving some of the lower states unoccupied. Accordingly, the occupation is described by an equilibrium Fermi-Dirac distribution with a global Fermi level for all electron levels.

When the temperature is reduced, the carriers are still uniformly distributed among the individual dots. However, thermal excitations freeze out, the nonradiative losses decrease, and charge-carrier condensation into the globally lowest-energy state occurs. This maximizes the occupation numbers of the GS and ES transitions.

At even lower temperatures, this common occupation statistics or global equilibrium collapses. The exchange of carriers between the individual dots breaks down and inside each dot all the energetically lowest states have the same

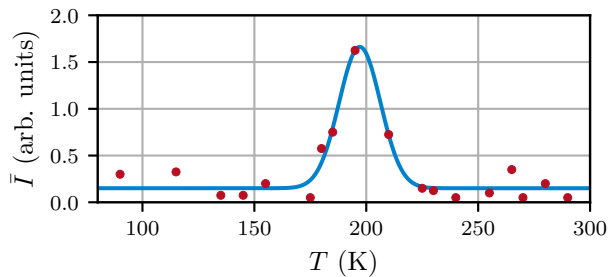


FIG. 4. Mean output intensity \bar{I} vs temperature T . Experimental data (red, Ref. [59]) and model [blue, Eq. (10)] yield a maximum intensity at around 190 K, implying an increase in diode efficiency at this temperature.

population, irrespective of their energy. This characterizes a so-called random population. The resulting distribution is a nonequilibrium distribution with a “virtual” excitation spectrum obtained by averaging over the whole ensemble, thus reflecting more the energetically inhomogeneous dot distribution. This leads again to a decrease in radiative recombination accompanied by a small increase in linewidth.

In essence, at around 190 K, a maximum in the radiative recombination occurs due to the occupation condensation into the globally lowest-lying state that is still described by a Fermi-Dirac distribution. This redistribution of carriers modifies the optical gain properties of the QDSDL that we investigate through temperature-resolved spectral analysis. The spectral peak power extracted from the maximum value of the optical spectra represents an easily accessible indicator for the spectral gain.

The relative development of the peak power is shown in Fig. 4. In the weakly coupled thermal regime at 190 K, we find an increase in peak power compared to room temperature due to the condensation of charge carriers. The local maximum in peak power indicates a larger amplification, which in turn affects the photon emission process. At room temperature, the QDSDL emits amplified spontaneous emission in a delicate balance, where spontaneously emitted photons are amplified moderately. At 190 K, the maximum in the spectral gain increases the probability of stimulated emission such that the initial spontaneous emission experiences a stronger amplification. These quasistimulated processes reduce the second-order intensity correlation coefficient $g^{(2)}(0)$ and suppress intensity fluctuations [60,61], thus realizing the exciting hybrid coherent characteristics of the emission.

The consequence of this behavior is a hierarchy in the contributing QD levels with a peak behavior of the emitted intensity as a function of temperature as illustrated by Fig. 4, which shows the experimental findings of the emitted intensity of the diode as a function of temperature. We can phenomenologically model the emitted power as a temperature-dependent Gaussian function with an offset δI ,

$$\bar{I}(T) = \bar{I}e^{-(T-T_0)^2/\sigma^2} + \delta I. \quad (10)$$

The experimental data can be fitted well for $\bar{I} = 1.51 \pm 0.13$, $T_0 = (197.1 \pm 0.9)$ K, $\sigma = (13.1 \pm 1.0)$ K, and $\delta I = 0.15 \pm 0.03$.

These thermal fitting parameters can be used to construct the temperature-dependent behavior of $g^{(2)}[0, \bar{I}(T)]$. As can

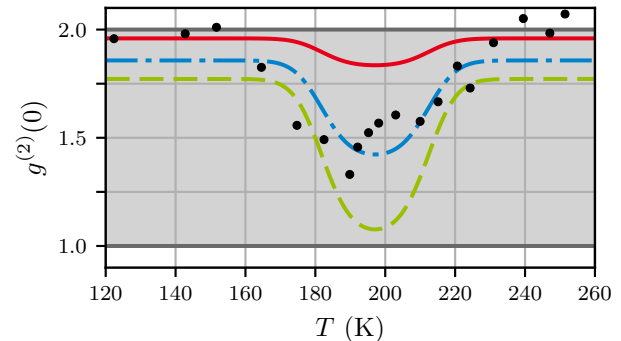


FIG. 5. Second-order correlation coefficient $g^{(2)}[0, \bar{I}(T)]$ vs temperature T for $I_s = 5$ and varying saturation parameter values κ . For $\kappa = 0.35$ (blue, dashed-dotted), we are able to match the experimental data [34]. This agreement deteriorates for $\kappa = 0.1$ (red, solid). Within the limits of the model, the intensity noise suppression could even reach $g^{(2)}(0) = 1.07$ for $\kappa = 0.56$ (green, dashed).

be seen in Fig. 5, all nonlinear saturation parameter combinations κ show a suppression of intensity fluctuations around 190 K. With the parameters set to $I_s = 5$ and $\kappa = 0.35$ (blue), we achieve good agreement with the experimental data [34]. The calculations using the fitted data from Fig. 4 do not reach a plateau of $g^{(2)}(0) = 2.0$ for high and low temperatures. This is due to the finite offset $\delta I = 0.15 \pm 0.03$ of $\bar{I}(T)$. With the saturation parameters set to $I_s = 5$ and $\kappa = 0.56$ (green), we are able to produce an intensity noise suppression below the experimentally reported value of $g^{(2)}(0) = 1.33$ with a minimum of about $g^{(2)}(0) = 1.07$.

Having developed a good description of the experimentally observed $g^{(2)}(0)$ reduction of hybrid light, we are now able to search towards even more reduction, eventually reaching the Poissonian correlation limit of $g^{(2)} = 1$, still keeping the spectral broadband character. Adjusting our model parameters, we are able to show reductions of $g^{(2)}(0)$ nearly down to a value of 1.07 for a $\kappa = 0.56$, very close to “real” Poissonian statistics, but now not for a laser but still for a broadband hybrid ASE light source. However, we admit that it is experimentally and technologically quite challenging to find appropriate QD level systems and QDSDL designs preventing stimulated modal emission, thus maintaining low first-order coherence, and avoiding a collapse of the spectral linewidth [35].

In conclusion, we have developed a quantum optical model for a thermally tuned photon statistics transformation of broadband THz-wide ASE radiation emitted from a quantum dot superluminescent diode from the thermal Bose-Einstein statistics towards Poissonian statistics, thus producing silent white light. The two ingredients, nonlinear gain saturation and an increased recombination determined by the temperature dependence of the hierarchy of the quantum dot occupation, allowed to account for the experimentally observed findings considering real world parameters. This is relevant for a variety of applications, such as optical coherence tomography [37,38,49], white light interferometry [50–52], control of chemical kinetics with tailored incoherent light [53], or sensing with fiber optic gyroscopes [54,55].

The data that support the findings of this study are available from the contact author upon reasonable request.

We gratefully acknowledge supporting discussions with Dr. Martin Blazek. R.W. and K.N.H. are supported by the DLR German Aerospace Center with funds provided by the Federal Ministry for Economic Affairs

and Climate Action (BMWK) due to an enactment of the German Bundestag under Grant No. 50WM2250E (QUANTUS+).

The authors have no conflict of interest to disclose.

- [1] R. Pike, Lasers, photon statistics, photon-correlation spectroscopy and subsequent applications, *J. Eur. Opt. Soc.-Rapid Publ.* **5**, 10047s (2010).
- [2] C. Beenakker and C. Schönberger, Quantum shot noise, *Phys. Today* **56**(5), 37 (2003).
- [3] R. Loudon, *The Quantum Theory of Light*, 3rd ed. (Oxford University Press, Oxford, UK, 2009).
- [4] R. Hanbury Brown and R. Q. Twiss, Correlation between photons in two coherent beams of light, *Nature (London)* **177**, 27 (1956).
- [5] It is important to note that the Hanbury Brown and Twiss experiment was originally conceived to exploit correlations of fluctuations for the determination of star diameters [4].
- [6] W. Martienssen and E. Spiller, Coherence and fluctuations in light beams, *Am. J. Phys.* **32**, 919 (1964).
- [7] F. T. Arecchi, Measurement of the statistical distribution of Gaussian and laser sources, *Phys. Rev. Lett.* **15**, 912 (1965).
- [8] A. Gatti, D. Magatti, and F. Ferri, Three-dimensional coherence of light speckles: Theory, *Phys. Rev. A* **78**, 063806 (2008).
- [9] D. Magatti, A. Gatti, and F. Ferri, Three-dimensional coherence of light speckles: Experiment, *Phys. Rev. A* **79**, 053831 (2009).
- [10] M. Bertolitti, B. Crosignani, and P. di Porto, On the statistics of Gaussian light scattered by a Gaussian medium, *J. Phys. A: Gen. Phys.* **3**, L37 (1970).
- [11] K. A. O'Donnell, Speckle statistics of doubly scattered light, *J. Opt. Soc. Am.* **72**, 1459 (1982).
- [12] D. W. Schaefer and P. N. Pusey, Statistics of non-Gaussian scattered light, *Phys. Rev. Lett.* **29**, 843 (1972).
- [13] E. Jakeman and P. N. Pusey, Significance of K distributions in scattering experiments, *Phys. Rev. Lett.* **40**, 546 (1978).
- [14] P. Lodahl, A. P. Mosk, and A. Lagendijk, Spatial quantum correlations in multiple scattered light, *Phys. Rev. Lett.* **95**, 173901 (2005).
- [15] S. Hartmann, F. Friedrich, A. Molitor, M. Reichert, W. Elsässer, and R. Walser, Tailored quantum statistics from broadband states of light, *New J. Phys.* **17**, 043039 (2015).
- [16] M. Kindermann, Y. V. Nazarov, and C. W. J. Beenakker, Manipulation of photon statistics of highly degenerate incoherent radiation, *Phys. Rev. Lett.* **88**, 063601 (2002).
- [17] S. Balog, P. Zakharov, F. Scheffold, and S. E. Skipetrov, Photocount statistics in mesoscopic optics, *Phys. Rev. Lett.* **97**, 103901 (2006).
- [18] H. E. Kondakci, A. Szameit, A. F. Abouraddy, D. N. Christodoulides, and B. E. A. Saleh, Sub-thermal to super-thermal light statistics from a disordered lattice via deterministic control of excitation symmetry, *Optica* **3**, 477 (2016).
- [19] J. Mork and K. Yvind, Squeezing of intensity noise in nanolasers and nanoLEDs with extreme dielectric confinement, *Optica* **7**, 1641 (2020).
- [20] H. E. Kondakci, A. F. Abouraddy, and B. E. A. Saleh, Lattice topology dictates photon statistics, *Sci. Rep.* **7**, 8948 (2017).
- [21] H. E. Kondakci, A. Szameit, A. F. Abouraddy, D. N. Christodoulides, and B. E. A. Saleh, Interferometric control of the photon-number distribution, *APL Photonics* **2**, 071301 (2017).
- [22] D. F. Walls, Evidence for the quantum nature of light, *Nature (London)* **280**, 451 (1979).
- [23] U. L. Andersen, T. Gehring, C. Marquardt, and G. Leuchs, 30 years of squeezed light generation, *Phys. Scr.* **91**, 053001 (2016).
- [24] D. B. Horoshko, M. I. Kolobov, F. Gumpert, I. Shand, F. König, and M. V. Chekhova, Nonlinear Mach-Zehnder interferometer with ultrabroadband squeezed light, *J. Mod. Opt.* **67**, 41 (2020).
- [25] E. S. Polzik, J. Carri, and H. J. Kimble, Spectroscopy with squeezed light, *Phys. Rev. Lett.* **68**, 3020 (1992).
- [26] H. Vahlbruch, M. Mehmet, S. Chelkowski, B. Hage, A. Franzen, N. Lastzka, S. Goßler, K. Danzmann, and R. Schnabel, Observation of squeezed light with 10-dB quantum-noise reduction, *Phys. Rev. Lett.* **100**, 033602 (2008).
- [27] J. Aasi, J. Abadie, B. P. Abbott, R. Abbott, T. D. Abbott, M. R. Abernathy, C. Adams, T. Adams, P. Addesso, R. X. Adhikari *et al.*, Enhanced sensitivity of the LIGO gravitational wave detector by using squeezed states of light, *Nat. Photon.* **7**, 613 (2013).
- [28] A. P. Foster, D. Hallett, I. V. Iorsh, S. J. Sheldon, M. R. Godland, B. Royall, E. Clarke, I. A. Shelykh, A. M. Fox, M. S. Skolnick *et al.*, Tunable photon statistics exploiting the Fano effect in a waveguide, *Phys. Rev. Lett.* **122**, 173603 (2019).
- [29] Y. Yamamoto, S. Machida, and W. H. Richardson, Photon number squeezed states in semiconductor lasers, *Science* **255**, 1219 (1992).
- [30] S. Machida, Y. Yamamoto, and Y. Itaya, Observation of amplitude squeezing in a constant-current-driven semiconductor laser, *Phys. Rev. Lett.* **58**, 1000 (1987).
- [31] S. M. Ulrich, C. Gies, S. Ates, J. Wiersig, S. Reitzenstein, C. Hofmann, A. Löffler, A. Forchel, F. Jahnke, and P. Michler, Photon statistics of semiconductor microcavity lasers, *Phys. Rev. Lett.* **98**, 043906 (2007).
- [32] A. Allevi and M. Bondani, Direct detection of super-thermal photon-number statistics in second-harmonic generation, *Opt. Lett.* **40**, 3089 (2015).
- [33] A. Allevi, S. Cassina, and M. Bondani, Super-thermal light for imaging applications, *Quantum Meas. Quantum Metrol.* **4**, 26 (2017).
- [34] M. Blazek and W. Elsässer, Coherent and thermal light: Tunable hybrid states with second-order coherence without first-order coherence, *Phys. Rev. A* **84**, 063840 (2011).
- [35] S. Hartmann, A. Molitor, M. Blazek, and W. Elsässer, Tailored first- and second-order coherence properties of quantum dot superluminescent diodes via optical feedback, *Opt. Lett.* **38**, 1334 (2013).

- [36] S. Hartmann and W. Elsässer, A novel semiconductor-based, fully incoherent amplified spontaneous emission light source for ghost imaging, *Sci. Rep.* **7**, 41866 (2017).
- [37] M. Blazek, S. Hartmann, A. Molitor, and W. Elsaesser, Unifying intensity noise and second-order coherence properties of amplified spontaneous emission sources, *Opt. Lett.* **36**, 3455 (2011).
- [38] D. Huang, E. A. Swanson, C. P. Lin, J. S. Schuman, W. G. Stinson, W. Chang, M. R. Hee, T. Flotte, K. Gregory, C. A. Puliafito, and J. G. Fujimoto, Optical coherence tomography, *Science* **254**, 1178 (1991).
- [39] K. Böhm, R. Ulrich, P. Russer, and E. Weidel, Low-noise fiber-optic rotation sensing, *Opt. Lett.* **6**, 64 (1981).
- [40] T. B. Pittman, Y. H. Shih, D. V. Strekalov, and A. V. Sergienko, Optical imaging by means of two-photon quantum entanglement, *Phys. Rev. A* **52**, R3429(R) (1995).
- [41] A. Gatti, M. Bache, D. Magatti, E. Brambilla, F. Ferri, and L. A. Lugiato, Coherent imaging with pseudo-thermal incoherent light, *J. Mod. Opt.* **53**, 739 (2006).
- [42] F. Friedrich, Hybrid coherent light - Modeling light-emitting quantum dot superluminescent diodes, Ph.D. thesis, Technische Universität Darmstadt, 2019, <https://tuprints.ulb.tu-darmstadt.de/8527>.
- [43] F. Friedrich, W. Elsässer, and R. Walser, Emission spectrum of broadband quantum dot superluminescent diodes, *Opt. Commun.* **458**, 124449 (2020).
- [44] K. N. Hansmann and R. Walser, Stochastic simulation of emission spectra and classical photon statistics of quantum dot superluminescent diodes, *J. Mod. Phys.* **12**, 22 (2021).
- [45] I. V. Doronin, E. S. Andrianov, A. A. Zyablovsky, A. A. Pukhov, Y. E. Lozovik, A. P. Vinogradov, and A. A. Lisyansky, Second-order coherence properties of amplified spontaneous emission, *Opt. Express* **27**, 10991 (2019).
- [46] R. Walser and P. Zoller, Laser-noise-induced polarization fluctuations as a spectroscopic tool, *Phys. Rev. A* **49**, 5067 (1994).
- [47] H. Huang and D. Deppe, Rate equation model for nonequilibrium operating conditions in a self-organized quantum-dot laser, *IEEE J. Quantum Electron.* **37**, 691 (2001).
- [48] A. E. Zhukov, V. M. Ustinov, A. Y. Egorov, A. R. Kovsh, A. F. Tsatsulnikov, N. N. Ledentsov, S. V. Zaitsev, N. Y. Gordeev, P. S. Kopev, and Z. I. Alferov, Negative characteristic temperature of InGaAs quantum dot injection laser, *Jpn. J. Appl. Phys.* **36**, 4216 (1997).
- [49] M. Blazek and W. Elsässer, Emission state hierarchy governed coherence and intensity noise properties of quantum dot superluminescent diodes, *IEEE J. Quantum Electron.* **48**, 1578 (2012).
- [50] E. N. Leith and G. J. Swanson, Achromatic interferometers for white light optical processing and holography, *Appl. Opt.* **19**, 638 (1980).
- [51] K. Naganuma, K. Mogi, and H. Yamada, Group-delay measurement using the Fourier transform of an interferometric cross correlation generated by white light, *Opt. Lett.* **15**, 393 (1990).
- [52] T. V. Amotchkina, A. V. Tikhonravov, M. K. Trubetskov, D. Grupe, A. Apolonski, and V. Pervak, Measurement of group delay of dispersive mirrors with white-light interferometer, *Appl. Opt.* **48**, 949 (2009).
- [53] F. O. Laforge, M. S. Kirschner, and H. A. Rabitz, Shaped incoherent light for control of kinetics: Optimization of up-conversion hues in phosphors, *J. Chem. Phys.* **149**, 054201 (2018).
- [54] S. Zheng, M. Ren, X. Luo, H. Zhang, and G. Feng, Real-time compensation for SLD light-power fluctuation in an interferometric fiber-optic gyroscope, *Sensors* **23**, 1925 (2023).
- [55] V. M. Passaro, A. Cuccovillo, L. Vaiani, M. De Carlo, and C. E. Campanella, Gyroscope technology and applications: A review in the industrial perspective, *Sensors* **17**, 2284 (2017).
- [56] C. Cohen-Tannoudji, J. Dupont-Roc, and G. Grynberg, *Atom-Photon Interactions* (Wiley-VCH, Weinheim, Germany, 1998).
- [57] P. Meystre and M. Sargent, *Elements of Quantum Optics* (Springer, Berlin, 2007).
- [58] F. W. J. Olver, A. B. Olde Daalhuis, D. W. Lozier, B. I. Schneider, R. F. Boisvert, C. W. Clark, B. R. Miller, B. V. Saunders, H. S. Cohl, and M. A. McClain, NIST Digital Library of Mathematical Functions, <http://dlmf.nist.gov/>, release 1.1.9 of 2023 March 15.
- [59] M. Blazek, Thermisch und kohärent: Erzeugung neuartiger Lichtzustände mittels Quantenpunkt-Superlumineszenzdioden, Ph.D. thesis, Technische Universität Darmstadt, 2011, <https://tuprints.ulb.tu-darmstadt.de/3079/>.
- [60] M. Blazek, S. Breuer, T. Gensty, W. E. Elsässer, M. Hopkinson, K. M. Groom, M. Calligaro, P. Resneau, and M. Krakowski, Intensity noise of ultrabroadband quantum dot light emitting diodes and lasers at 1.3 μm , *Proc. SPIE* **6603**, 66031Y (2007).
- [61] S. Shin, U. Sharma, H. Tu, W. Jung, and S. A. Boppart, Characterization and analysis of relative intensity noise in broadband optical sources for optical coherence tomography, *IEEE Photonics Technol. Lett.* **22**, 1057 (2010).